Nuclear Instruments and Methods in Physics Research B 554 (2024) 165442

Contents lists available at ScienceDirect

Nuclear Inst. and Methods in Physics Research, B

journal homepage: www.elsevier.com/locate/nimb

On the question whether surface roughness can explain the absence of a prominent single-collision peak in keV heavy-ion scattering off a polycrystalline Ru surface

L. Assink [a,b], J. Brötzner [c], C. Cupak [c], M. Salverda [a,b], H.T. Jonkman [a], O.O. Versolato [b,d], R.A. Wilhelm [c], R. Hoekstra [a,b,*]

[a] Zernike Institute for Advanced Materials, University of Groningen, Nijenborgh 4, 9747 AG, Groningen, The Netherlands
[b] Advanced Research Center for Nanolithography (ARCNL), Science Park 106, 1098 XG, Amsterdam, The Netherlands
[c] Institute of Applied Physics, TU Wien, Wiedner Hauptstr. 8-10/E134, 1040, Vienna, Austria
[d] Department of Physics and Astronomy, and LaserLaB, Vrije Universiteit, De Boelelaan 1081, 1081 HV, Amsterdam, The Netherlands

ARTICLE INFO

Keywords:
Heavy ions
Ion scattering
Binary collision approximation
Surface roughness

ABSTRACT

In a joint experimental and modeling effort, we have studied 15 keV Ar^{2+}, Kr^{2+}, and Xe^{2+} projectiles scattering off a polycrystalline Ru surface to assess the possible role of surface roughness in the apparent near-absence of the single-collision (SC) peak for Xe, the heaviest of the ions. The surface roughness of the Ru sample was determined by atomic force microscopy (AFM). The AFM image is used as input to simulations by means of the ray tracing code SPRAY. The observed spectra display a significant SC peak in the energy distributions of reflected Ar and Kr ions, which is not the case for Xe. The energy spectrum produced by the reflection of Xe and recoiled Ru ions closely corresponds to the results obtained from our SPRAY simulations. It is evident that surface roughness plays a crucial role in the visibility of the SC peak. From simulations for different target roughnesses, it is clear that a concentrated distribution of inclination angles centered around 2° effectively reduces the intensity of the single-collision peak for Xe ion scattering. The presence of a distinct SC peak for Ar and Kr ions, unlike Xe ions, supports the notion that the absence of a prominent SC peak in Xe ion scattering is not primarily due to geometric blocking of trajectories by surface roughness. This suggests that for slow, heavy ions like Xe, scattering effects arising from the nearest neighbors to the binary collision partner are significant and should be carefully examined.

1. Introduction

To model what happens when keV ions impact on a surface, binary collision codes like SRIM [1,2] are typically used. The output of these codes has been extensively tested [3–5] for the reflection of light ions at these low energies, as it finds an application in analysis methods such as low-energy ion scattering (LEIS) [6–8]. However, data on the interaction between keV heavy ion scattering and a heavy surface appears to be lacking. Recently, an extensive systematic study of the interaction of Sn ions on the transition metals Mo and Ru was performed [9]. While the experimental data did not show a clear sign of a single binary collision (SC) peak on top of the broad multiple-scattering distribution, all tested binary codes did show the peak, though intensities varied between different simulation packages. Many options were considered to explain the absence or extensive smearing out of the SC peak such that it is no longer visible on top of the multiple-scattering background.

A possible explanation not rigorously tested yet is surface roughness. In this joint experimental and modeling study, we investigate whether surface roughness may be the cause of the apparent absence of the SC peak. If roughness-induced blocking of ion trajectories would suppress the SC peak for specific scattering angles, the choice of projectile should not matter. To test this, we considered noble gas projectile ions, i.e. Ar, Kr, and Xe, which substitute for Sn ions used in our previous work [9]. Xe ions are more conveniently produced than Sn ions and in higher beam currents. Kinetic energy distributions of reflected Ar, Kr, and Xe particles are measured with an electrostatic analyzer. The results are discussed in comparison to SPRAY simulations. The SPRAY code is a ray-tracing code that explicitly includes surface roughness. The surface roughness is extracted from atomic force microscopy (AFM) images of the surface. The collisions are described by conventional binary collision approximations.

* Corresponding author at: Zernike Institute for Advanced Materials, University of Groningen, Nijenborgh 4, 9747 AG, Groningen, The Netherlands.
E-mail address: r.a.hoekstra@rug.nl (R. Hoekstra).

https://doi.org/10.1016/j.nimb.2024.165442
Received 25 April 2024; Received in revised form 31 May 2024; Accepted 13 June 2024
Available online 24 June 2024

Using the comparison of SPRAY simulations and experimental data together with the spectral differences between the results of Ar, Kr, and Xe ions, it is argued that it is unlikely that the absence of the SC peak for heavy projectiles such as Xe (and Sn) is primarily a result of geometrical blocking of SC trajectories due to roughness. In addition, the remarkable large fraction of energetic Ru recoils stemming from binary single collision events is discussed.

2. Research methods

2.1. Experimental setup

The primary beams of 15 keV Ar^{2+}, Kr^{2+}, and Xe^{2+} are extracted from the 14-GHz Electron Cyclotron Resonance (ECR) ion source (SUPERNANOGAN, Pantechnik) at the ZERNIKELEIF ion beam facility at the University of Groningen. An 110° analyzing magnet with a resolution of ~0.5% assures the use of monoisotopic ion beams: ^{40}Ar, ^{84}Kr, and ^{132}Xe. By means of three magnetic quadrupole triplets, the ion beam is transported 15 m downstream. For final mass-over-charge clean up, a 45° dipole magnet is placed 2 m in front of the collision chamber. Since the main components of the setup are presented in detail in previous papers [10–12], only a brief description of the setup is given here. The polycrystalline Ru target (Surface Preparation Labs, Zaandam, The Netherlands) is attached to the sample holder of a five-axes manipulator mounted on top of a μ-metal chamber kept at a base pressure of 10^{-10} mbar. By rotating the target around its axis, the angle of incidence with respect to the surface plane, ψ, can be set with a resolution of 0.1°. In the present experiments, the incidence angle is kept constant at 15°. The rotatable high-precision electrostatic analyzer (ESA), which measures ions only, is used at a scatter angle of $\theta = 40°$. The ESA has an opening diaphragm of 0.4 mm, positioned 75 mm from the sample, which allows for a solid angle $\Delta\Omega$ of $2.2 \cdot 10^{-5}$ sr at the center of the target. Each ESA spectrum presented here is corrected for the beam current, the solid angle, the increasing energy bin size resulting from the spectrometer's fixed $\Delta E/E$ resolution (0.5% FWHM), and the energy-dependent detection efficiency of the microchannel plate. For the latter correction, the empirical detection efficiency curves determined by Krems et al. [13] are used. Given the energy range of reflected Ar, Kr, and Xe ions, i.e. approximately 6–10 keV, only a small correction for the lowest-energy Xe ions of at most ~20% is needed to be applied.

To assess the roughness of the Ru sample, the sample was taken out of the collision chamber and transferred to a Bruker Dimension ICON Atomic Force Microscope (AFM). A typical AFM topographical image of 4 μm^2 of the Ru surface after Ar sputtering and heat treatment is shown in Fig. 1. Outside of the deeper troughs, which are remnants of the original surface polishing, the sample locally has an RMS roughness of 0.7 nm. This RMS roughness is taken over an area of 0.3 μm^2. The sample is oriented such that the troughs are aligned along the detector plane. This way, projectile ions that impinge on the sidewalls of the troughs are scattered out of the detector plane, and thus do not contribute to the experimental results. It is to be realized that for the treated sample, shown in Fig. 1, the side walls are inclinated to the surface plane by at maximum 5° to 10° (see also Fig. 3).

2.2. Binary collision approximation (BCA)

For a binary collision of a projectile of mass m_p with energy E_0 on a target atom of mass m_t the final energy E_f after scattering over an angle θ is given by:

$$E_f = \left(\frac{\cos(\theta) \pm \sqrt{(m_t/m_p)^2 - \sin^2(\theta)}}{1 + m_t/m_p} \right)^2 E_0. \quad (1)$$

The energy of a recoiled target particle E_{rec} detected at the same scattering angle θ is given by:

$$E_{rec} = \frac{4 m_t m_p}{(m_t + m_p)^2} \cos^2(\theta)\, E_0. \quad (2)$$

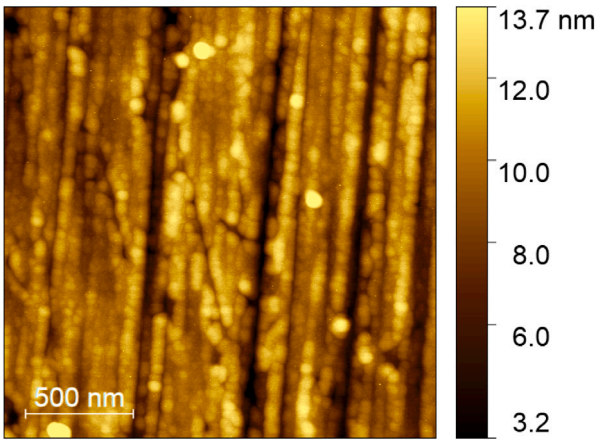

Fig. 1. A typical 2 × 2 μm^2 AFM topography image of the polycrystalline Ru surface being exposed to Ar ion beam cleaning and heat treatment. The 10-nm height scale is shown by the color bar on the right.

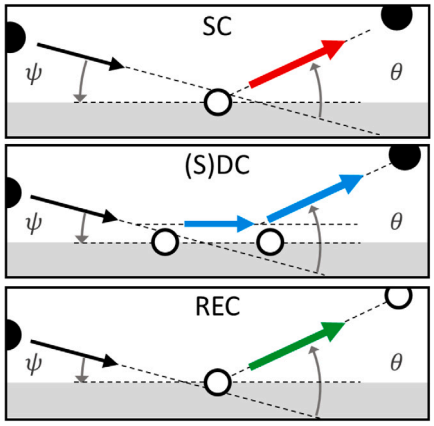

Fig. 2. Visualization and color coding of different collisional events leading to the detection of a particle at a scattering angle θ. For a given projectile impinging under an incidence angle ψ, three types of collision processes are considered: top panel — single collisions (SC), middle panel — (symmetric) double collisions ((S)DC), and primary target recoils (REC). In all other figures, the positions of SC, (S)DC, and REC events will be indicated by red, blue and green bars, respectively.

The ± sign in Eq. (1) takes care of the two options for a heavier particle scattering on a lighter target atom. Here, this is relevant to the Xe-Ru collision system. The projectile being heavier than the target atom also implies that there is a maximum scattering angle that can be reached. The maximum scattering angle is then calculated by $\theta_{max} = \arcsin(m_t/m_p)$, which yields for ^{132}Xe projectiles on Ru a maximum angle of approximately 50°, assuming a weighted average mass of Ru of 101.1 mass units.

In the comparison between experiments and model simulations, we will mainly focus on the three different types of scattering events, which are depicted in Fig. 2.

- Single collision (SC): the projectile is deflected over an angle θ after colliding only once with a target atom. If roughness would geometrically block SC trajectories from reaching the detector, it would affect all ions (Ar, Kr, and Xe) alike.
- Double collision (DC): the projectile is deflected over an angle θ after two consecutive collisions with a target atom. From Eq. (1) it follows that, in total, less energy is lost by the projectile when it scatters twice, thus if $\theta_1 + \theta_2 = \theta$, with θ_1 and θ_2 the scattering angles of the first and second collision, respectively. The least energy is lost in symmetric double collisions (SDC), i.e. $\theta_1 =$

$\theta_2 = \theta/2$. However, as can be inferred from Fig. 2, symmetric double collisions can only occur if the incidence angle $\psi > \theta/2$. Otherwise, the particle would already be scattered away from the surface after the first scattering event. No symmetric double collisions will take place unless the target is locally rough.

- Primary target recoils (REC): an energetic target atom knocked out of the sample by the projectile in a single collision. In order to do so, the projectile should hit the target atom from below the surface. The likelihood to do so depends on the incidence angle ψ and once again on the local roughness of the surface. At the relatively small angle of incidence of $\psi = 15°$ used here, roughness would likely enhance the production of primary target recoils.

In the results discussed in the next sections, the energy ranges in which the three types of collision events are expected to show up are indicated by shaded bands in the same color code as used in Fig. 2: SC — red, (S)DC — blue, and REC — green. The width of these bands is determined by the different masses of the Ru isotopes, and an angular scattering range of ±0.5°.

2.3. SPRAY simulations

The simulations described in this paper have been performed using the SPRAY code. As this code is explained in detail in [14], only a brief description of the working principles of the simulation package is given here. Where most conventional BCA codes assume a perfectly flat target, only a few include sample roughness [14–16]. The SPRAY code is a ray-tracing simulation code that is especially developed to study target sputtering and re-deposition in case of rough surfaces. SPRAY is based on a repository of energy-dependent scattering angle distributions pre-calculated with SDTrimSP [17] for the projectile target combination of interest. Thus, intrinsic features of SDTrimSP in describing the binary collision are part of SPRAY as well. In the present work we used the option of SDTrimSP to include weak collisions along the projectile trajectory. This explicit inclusion of nearest neighbor interactions upgrades the description from a pure binary case to the integral scattering off a small surface area. By triangulating a surface, the roughness in SPRAY is described as locally tilted surfaces. The code can incorporate the actual surface roughness of an experimental sample by importing an atomic force microscopy (AFM) image of that surface. This is in contrast to codes like TRI3DYN and SDTrimSP-3D, which build their surfaces as cubic voxels, leading to untilted flat surfaces on the size scale of the voxel dimensions. Instead of using the root mean square (RMS) value of the target roughness, SPRAY describes the surface roughness by means of the surface inclination angle distribution (SIAD) of flat surface patches (see inset Fig. 3). This kind of representation of surface roughness was shown to be more appropriate for modeling ion sputtering of rough targets [14].

In this paper, SPRAY simulations are performed for three targets, each with different sample roughness. Besides the ‘treated’ target as shown in Fig. 1, two other test targets are used. One of these targets is generated to be artificially flat. It represents the ideal scenario without any kind of roughness. As no roughness is present, the SPRAY simulations do not differ from conventional BCA codes. The roughest-surface scenario is based on an AFM image of the original Ru target before any kind of treatment. This target is referred to as the ‘untreated’ target. All the experimental results presented in this work were taken using the ‘treated’ target.

Fig. 3 compares the surface inclination angle distribution of the treated target (green) and untreated target (red). It is of note that the distribution of inclination angles of the treated target is limited to a few degrees only. Nevertheless, as will be shown, this suffices to affect the energy distributions of scattered projectiles. Simulations are performed for 15 keV Ar, Kr, and Xe beams incident at 15° on the flat, treated, and untreated Ru surface. The output of each of these simulations contains both reflected and recoiled particles. For an adequate comparison with enough statistics to the experiments on the treated target, the output of the simulations is binned in angular scattering and azimuthal bins of ±0.5° and ±4°, respectively, and an energy bin of 150 eV. The size of the angular scattering and azimuthal bins yield a solid angle $\Delta\Omega$ of $2.2 \cdot 10^{-3}$ sr.

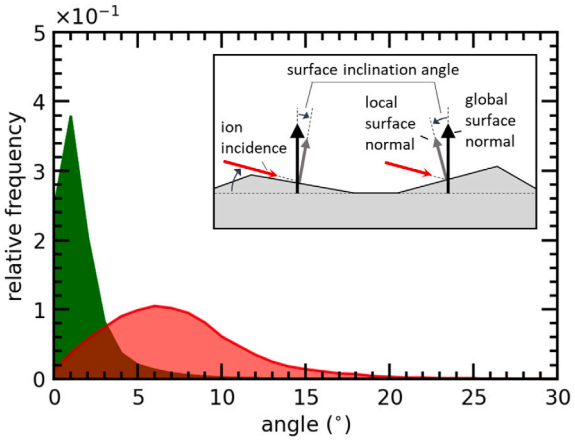

Fig. 3. The relative frequency of the absolute value of the surface inclination angle with respect to the global surface normal for the treated (green) and untreated (red) cases of surface roughness.

3. Results and discussion

3.1. Experimental results

Fig. 4 shows measured ion energy spectra taken with the ESA for 15 keV Ar^{2+} (left), Kr^{2+} (middle), and Xe^{2+} (right) ions colliding on the ‘treated’ Ru target at a scattering geometry of (ψ, θ) = (15°, 40°). The following general observations can be made on the contributions of SC, (S)DC, and REC to the spectrum.

Single collisions of Ar, Kr, and Xe projectiles

Looking at the energy distributions of the reflected ions, a prominent SC peak is seen for the 15 keV Ar and Kr projectiles. For the 15 keV Xe projectiles, a broad structure appears in the ion spectrum at and slightly above the SC-peak energy. The latter is likely due to hetero-atomic double collisions on O and Ru atoms. The maximum scattering angle of Xe on O is only 7°. For additional scattering on O over 2°, a peak would appear at ~7.4 keV in the ESA spectrum of Xe. The fact that the SC peaks are dominantly present for Ar and Kr ions indicates that roughness of the surface in our case does not lead to significant geometrical blocking of SC trajectories. For Xe ions, SC events show up in the spectrum but no clear SC peak stands out in the spectrum. This may in part be explained because of overlap with ions stemming from hetero-atomic double collisions and with a possible overlapping low-energy tail of Ru recoils. On top of that, the ion spectrum is measured at a scattering angle of $\theta = 40°$, which is not far below the maximum scattering angle for Xe on Ru of 50°. Thus, the cross section for scattering over 40° is expected to be small.

Double collisions of Ar, Kr, and Xe projectiles

The exact energies of the DC peak in the ESA spectra of, in particular, Kr and Xe underline the conclusion drawn from the SC results that the surface roughness does not play an appreciable part. The DC peaks fall just below the calculated energies of the symmetric double-collision peak marked by the dark blue bands in Fig. 4. For a scatter angle of $\theta = 40°$, an SDC peak requires two consecutive collisions of 20° to take

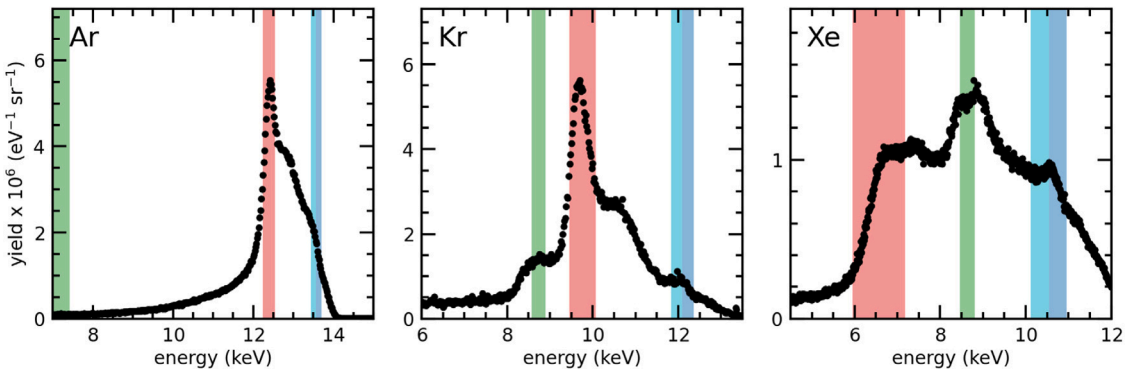

Fig. 4. Ion energy distributions of reflected projectile and recoiled target ions for 15 keV (left column) Ar^{2+}, (middle column) Kr^{2+}, and (right column) Xe^{2+} ions colliding on a Ru surface at a scattering geometry of (ψ, θ) = (15°, 40°). The expected energy range of the peak due to single collisions (red), double collisions (blue) and recoil (green) events are indicated by the shaded areas.

place. At an incoming angle of $\psi = 15°$, this is not possible unless local surface inclination in the surface exist (local surface roughness). For a locally flat surface, the DC events remaining the highest energy would show up for an angular combination of 15° and 25° scattering angles. The energy band associated with consecutive 15° and 25° scattering is indicated by the light blue bands in Fig. 4. It is indeed within the light blue bands that the DC peak primarily shows up.

Primary Ru recoils

Another interesting observation comes from the contribution of the primary Ru recoils (green-shaded areas). While the small fraction of Ru recoils does not interfere with the energy distribution of the reflected Ar ions, the larger contributions of Ru recoils for the heavier projectiles start to overlap with the energy distributions of the reflected ions. In particular for Xe: the distribution of the primary Ru recoils is in between the expected SC and (S)DC position, and thus, as mentioned above, a low-energy tail of primary Ru recoils may influence the shape of the energy spectrum near the position of the SC scattering events between 6 and 7 keV (see Fig. 4).

The presence of a primary recoil peak for Xe impact is in itself evidence that SC events take place. Primary recoils are the most energetic target particles knocked out of the sample by the projectile in a single collision. Contrary to single scattering, the projectile ions hit the target atom from below the surface. To knock out a Ru target atom over an angle θ of 40°, one finds by applying Eqs. (2) and (1) associated scatter angles of respectively 78°, 57°, and 41° for Ar, Kr, and Xe. Therefore, for the 40° angle under which the Ru recoils are measured here, Xe ions producing those primary recoils will be scattered over almost the same angle. Assuming that the Xe ions do not penetrate below the surface, one might expect intensities from SC Xe and recoiled Ru to be of similar magnitude.

3.2. SPRAY results

In Fig. 5, a compilation of the simulated energy spectra of reflected (magenta) and recoiled (green) particles is shown for 15 keV Ar (left column), Kr (middle column), and Xe (right column) projectiles incident on Ru targets of different sample roughness: flat target (top row), treated target (middle row), and the untreated target (bottom row). For all projectiles, the angle of incidence angle is $\psi = 15°$ with respect to the surface plane, and the scattering angle θ is 40°. The sum of both reflected and recoiled particles is shown for each of the cases by the grey shaded spectrum. Similarly as for the experimental spectra, the expected energy ranges of the three different collisional events (see Fig. 2) are in each spectrum highlighted by the corresponding colored bands.

Fig. 5 indicates that the overall yield decreases when the target roughness goes up. The decrease in intensity is similar for all three projectiles. This common behavior could be expected as a surface inclination distribution (roughness) leads to a larger angular range of outgoing trajectories almost independent of projectile species. Light ions might be a bit more sensitive since, for the same impact parameter, light particles get scattered over a larger angle, and therefore, compared to heavier projectiles, a bit more likely to be scattered out off the angular detection bin of the simulations (and experiments). When examining the simulated spectra of the perfectly flat target, depicted in the top row of Fig. 5, it is evident that an SC peak is detected at the anticipated energy for each of the projectile types. However, the effect of roughness on the SC peak appears to be very different for each projectile. Where the SC peak is only a little bit suppressed for the Ar projectile (left column), it gets fully suppressed for Xe (right column). Besides a suppressed SC peak, a similar suppression of the REC peak is observed. This suppression is particularly visible for the heavier projectiles, where the ratio between the SC peak and the REC peak is the smallest.

3.3. Comparison of experiment and simulation

For the treated Ru target, Fig. 6 compares normalized measured and simulated energy spectra. In comparing the measured and simulated spectra, one should realize that the measurements contain only charged particles, while in the simulations the charge state of the particles is not a parameter that is included. This difference might explain some of the (small) disagreements between the experiment and the simulation. From Fig. 6, one can see that for each projectile the low-energy tail is more pronounced in the simulated spectra than in the measured data. Typically, the tail is due to projectiles that scatter from deeper layers of the target and thus have a longer path length through the target which leads to enhanced straggling [18]. Generally, the lower the energy of the particle, the higher the probability that the scattered particles are neutralized [19].

For two of three projectiles (Ar and Xe) a good overall agreement between the experimental and simulation results is found. Interestingly enough, it is the Kr spectra where most disagreement is found. According to the SPRAY simulations, cf. Fig. 5, the shape of Ar spectrum is not very sensitive to the state of the surface roughness. On the contrary, the characteristic SC feature for Xe already disappears when going from the ideally flat to treated surface. For Kr, one notes that the SC peak is still present though less pronounced for the treated surface, and therefore

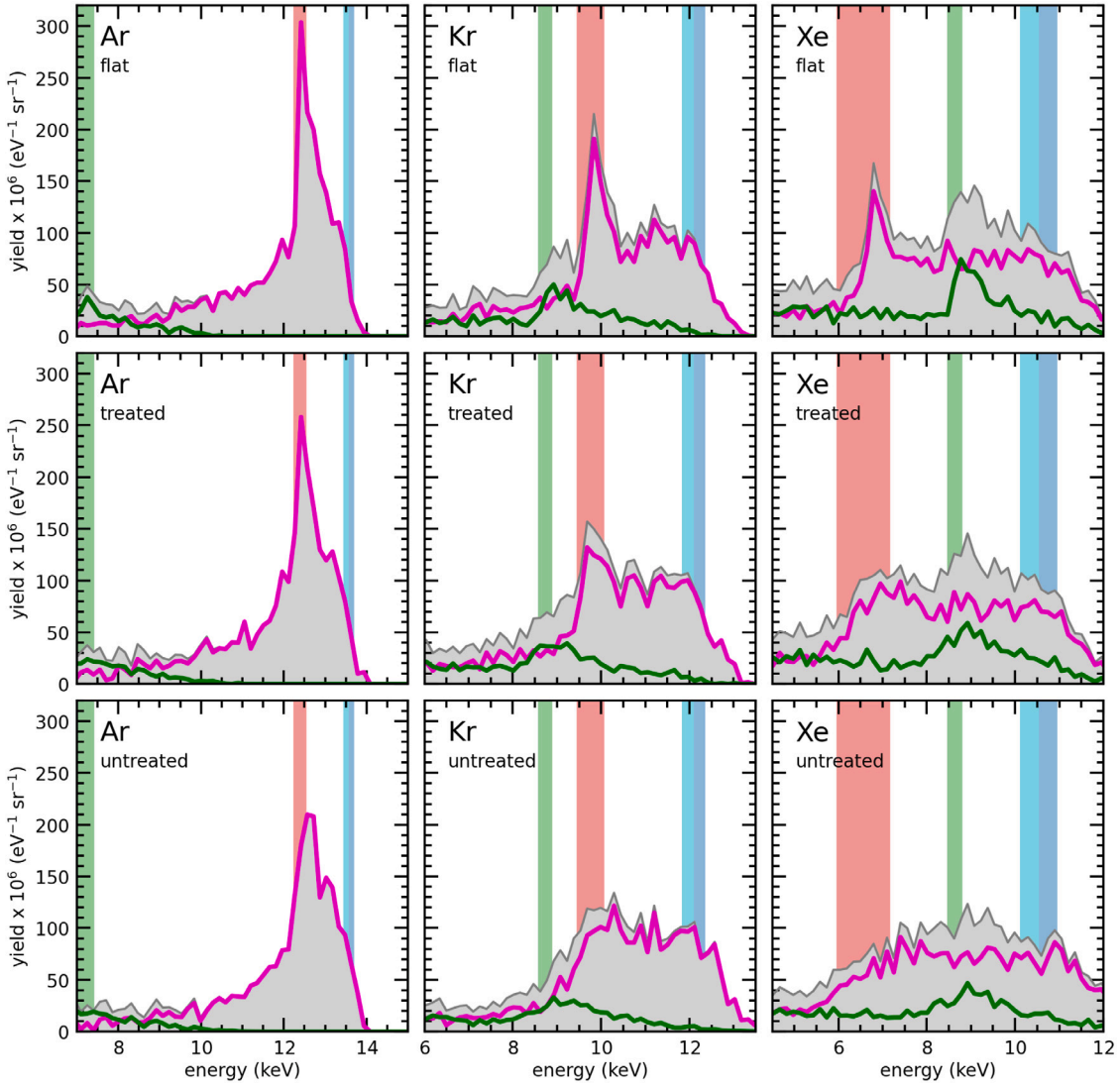

Fig. 5. Compilation of simulated energy distributions of reflected (magenta line) and recoiled (dark green line) particles for 15 keV Ar (left), Kr (middle), and Xe (right) projectiles colliding on Ru targets of different surface roughness: flat (top row), treated (middle row), and untreated (bottom row). For each case, the sum of the reflected and recoiled particles is shown by the grey shaded spectrum.

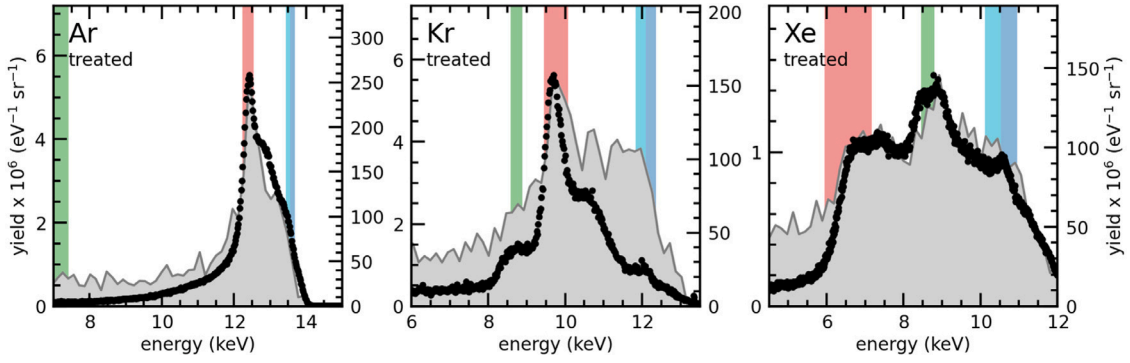

Fig. 6. Spectral comparison of the experimental ion yield (black, left axis) and simulated particle yield (grey, right axis) for 15 keV (left) Ar, (middle) Kr, and (right) Xe projectiles colliding on a Ru surface. The expected energy range of the peak due to single collisions (red), double collisions (blue) and primary recoils (green) are indicated by the shaded areas. A darker shade of blue is included in the double collision band to indicate the expected energy range of the symmetric double collisions.

might be most sensitive to the exact surface roughness. The area of the AFM image that served as input for the SPRAY simulations is smaller than the area from which scattered and recoiled ions are detected.

The high-energy side of the Kr spectrum, which contains the multiple scattering events, seems to be over-predicted by the simulations. However, one might equally well argue that the experimental spectrum is dominated by the SC events. The different ratio between SC and DC events in the simulations and the experiment could be due to a difference in the ion fractions for SC and DC trajectories, as assumed earlier for light ions [20]. This might be substantiated by the high ion fraction for Kr of ≈4% obtained from the ratio between the ion and particle yield. Future time-of-flight measurements, in which both ions and neutrals are measured, could help clarify a potential effect of different ionization fractions. According to the SPRAY simulations shown in Fig. 5, roughness appears an unlikely explanation for the measured low fraction of multiple collision events, as the intensity of the multiple scattering events is almost independent on the roughness.

4. Conclusion

We have conducted a concerted set of experiments and simulations to investigate keV heavy-ion scattering off a polycrystalline Ru surface. A possible explanation of surface roughness as the cause for the absence of a prominent SC peak for the heaviest ions was tested. Experimental ion energy spectra of reflected and recoiled ions were taken for 15 keV Ar^{2+}, Kr^{2+}, and Xe^{2+} projectile beams incident on the Ru target at a scattering geometry of $(\psi, \theta) = (15°, 40°)$. A clear SC peak was observed for Ar and Kr, while for Xe, a prominent SC peak remained to be absent. The shape of the combined energy spectrum of reflected Xe and recoiled Ru ions is very well reproduced by our SPRAY simulations. Input to the SPRAY calculations is the actual roughness of the surface, which is extracted from AFM images. The roughness is described by triangulating small surface patches which then obtain a slightly inclined angle (a few degrees at maximum) from the global target surface. It is found that roughness indeed strongly impacts the visibility of the SC peak. From comparison to simulations for an ideally flat sample surface, it is found that such a narrow distribution of inclination angles peaking around 2° suffices to wash out the SC peak for Xe ion scattering. The surface roughness in our case (cf. Fig. 1) is, however, too small to lead to geometrical blocking of certain trajectories. The observation of a clear SC peak for Ar and Kr, but not for Xe, is in support of the conclusion that roughness-induced geometrical blocking of trajectories is not the prime cause of the absence of a prominent peak for Xe ion scattering. Therefore, weak scattering events on nearest neighbors to the binary collision partner are decisive, because it are these nearest neighbor contributions that define the integral scattering on single surface area patches, which are used to construct the actual surface roughness.

CRediT authorship contribution statement

L. Assink: Writing – original draft, Visualization, Formal analysis, Data curation. **J. Brötzner:** Writing – review & editing, Software, Data curation. **C. Cupak:** Writing – review & editing, Software, Data curation. **M. Salverda:** Writing – review & editing, Resources, Investigation. **H.T. Jonkman:** Writing – review & editing, Resources, Investigation. **O.O. Versolato:** Writing – review & editing, Supervision. **R.A. Wilhelm:** Writing – review & editing, Validation, Supervision, Conceptualization. **R. Hoekstra:** Writing – review & editing, Supervision, Project administration, Methodology, Funding acquisition, Conceptualization.

Declaration of competing interest

The authors declare that they have no known competing financial interests or personal relationships that could have appeared to influence the work reported in this paper.

Data availability

Data will be made available on request.

Acknowledgments

This work was conducted as part of the research program of the Advanced Research Center for Nanolithography (ARCNL), a public–private partnership of the University of Amsterdam (UvA), Vrije Universiteit Amsterdam, University of Groningen (RuG), the Netherlands Organisation for Scientific Research (NWO), and the semiconductor equipment manufacturer ASML. The experiments were performed at the ZERNIKELEIF facility operated by the Zernike Institute for Advanced Materials at the University of Groningen. The SPRAY simulations were performed at the Institute of Applied Physics of the TU Wien.

References

[1] J.F. Ziegler, J.P. Biersack, U. Littmark, The Stopping and Range of Ions in Matter, Pergamon Press, New York, 1985.
[2] J.F. Ziegler, M.D. Ziegler, J.P. Biersack, SRIM – the stopping and range of ions in matter (2010), Nucl. Instrum. Methods Phys. Res. B 268 (11) (2010) 1818–1823.
[3] N. Novikov, Y. Teplova, Y. Fainberg, V. Kulikauskas, Reflection of nitrogen ions from copper surface: Experiment and calculations, Nucl. Instrum. Methods Phys. Res. B 235 (2005) 448–451.
[4] M. Jurado Vargas, A. Fernández Timón, A comparison between the codes SRIM and AlfaMC in the Monte Carlo simulation of alpha-particle backscattering, J. Radioanal. Nucl. Chem. 305 (479) (2015).
[5] V. Shulga, Note on the artefacts in SRIM simulations of sputtering, Appl. Surf. Sci. 439 (456) (2018).
[6] H. Brongersma, M. Draxler, M. de Ridder, P. Bauer, Surface composition analysis by low-energy ion scattering, Surf. Sci. Rep. 62 (2007) 63–109.
[7] C. Stilhano Vilas Boas, A. Zameshin, J. Sturm, F. Bijkerk, The influence of oxygen on the neutralization of slow helium ions scattered from transition metals and aluminum surfaces, Surf. Sci. 700 (2020) 121680.
[8] S. Průša, M. Linford, E. Vaníčková, P. Bábík, J. Pinder, T. Šikola, H. Brongersma, A practical guide to interpreting low energy ion scattering (LEIS) spectra, Appl. Surf. Sci. 657 (2024) 158793.
[9] R.A. Wilhelm, M.J. Deuzeman, S. Rai, W. Husinsky, P.S. Szabo, H. Biber, R. Stadlmayr, C. Cupak, J. Hundsbichler, C. Lemell, W. Möller, A. Mutzke, G. Hobler, O.O. Versolato, F. Aumayr, R. Hoekstra, On the missing single collision peak in low energy heavy ion scattering, Nucl. Instrum. Methods Phys. Res. B 544 (2023) 165123.
[10] S.T. de Zwart, A.G. Drentje, A.L. Boers, R. Morgenstern, Electron emission induced by multiply charged Ar ions impinging on a tungsten surface, Surf. Sci. 217 (1) (1989) 298–316.
[11] N. Stolterfoht, R. Hellhammer, D. Fink, B. Sulik, Z. Juhász, E. Bodewits, H.M. Dang, R. Hoekstra, Dynamic properties of ion guiding through nanocapillaries in an insulating polymer, Phys. Rev. A 79 (2009) 022901.
[12] E. Bodewits, H.M. Dang, A.J. de Nijs, D.F.A. Winters, R. Hoekstra, Atomic electron energy spectra of slow He^{2+} ions impinging on metallic surfaces, Nucl. Instrum. Methods Phys. Res. B 267 (4) (2009) 594–597.
[13] M. Krems, J. Zirbel, M. Thomason, R.D. DuBois, Channel electron multiplier and channelplate efficiencies for detecting positive ions, Rev. Sci. Instrum. 76 (2005) 093305.
[14] C. Cupak, P.S. Szabo, H. Biber, R. Stadlmayr, C. Grave, M. Fellinger, J. Brötzner, R.A. Wilhelm, W. Möller, A. Mutzke, M.V. Moro, F. Aumayr, Sputter yields of rough surfaces: Importance of the mean surface inclination angle from nano- to microscopic rough regimes, Appl. Surf. Sci. 570 (2021) 151204.
[15] W. Möller, TRI3DYN - collisional computer simulation of the dynamic evolution of 3-dimensional nanostructures under ion irradiation, Nucl. Instrum. Methods Phys. Res. B 322 (2014) 23–33.
[16] U. von Toussaint, A. Mutzke, A. Manhard, Sputtering of rough surfaces: a 3D simulation study, Phys. Scr. (2017) 014056.
[17] A. Mutzke, R. Schneider, W. Eckstein, R. Dohmen, SPTrimSP Version 5.00, IPP-Report 12/8, 2011, pp. 1–70.
[18] S. Lohmann, R. Holenák, P. Grande, D. Primetzhofer, Trajectory dependence of electronic energy-loss straggling at kev ion energies, Phys. Rev. B 107 (8) (2023) 085110.
[19] A. Boers, Charge state of low energy reflected particles, Nucl. Instrum. Methods Phys. Res. B 4 (1) (1984) 98–106.
[20] D. Primetzhofer, S. Rund, D. Roth, D. Goebl, P. Bauer, Electronic excitations of slow ions in a free electron gas metal: Evidence for charge exchange effects, Phys. Rev. Lett. 107 (16) (2011) 163201.